

Self-Organisation in 2D Swarms.

Jihad Touma,¹ Amer Shreim,² and Leonid I. Klushin³

¹*Center for Advanced Mathematical Studies (CAMS) and Physics Department, American University of Beirut, Beirut, Lebanon.**

²*Physics Department, American University of Beirut, Beirut, Lebanon.†*

³*American University of Beirut, Department of Physics, Beirut, Lebanon*
(Dated: June 19, 2018)

We undertake a systematic numerical exploration of self-organised states in a deterministic model of interacting, self-propelled particles in 2D. In the process, we identify new types of collective motion, namely disordered swarms, rings and droplets. We construct a “phase diagram”, which summarizes our results as it delineates phase transitions (all discontinuous) between disordered swarms and vortical flocks on one hand, and bound vortical flocks and expanding formations on the other. One of transition lines is found to have a close analogy in the temperature-driven gas-liquid transition in finite clusters with the same interparticle potential. Furthermore, we report on a novel type of flocking which takes place in the presence of a uniform external driver. Altogether, our results set a rather firm stage for experimental refinement and/or falsification of this class of models.

PACS numbers: 05.65.+b

Populations of self-propelled organisms tend to organize in remarkable aggregate formations [1]. Schools of fish, flocks of birds, swarms of bees or locust are among the more familiar examples. Less familiar perhaps, though equally prevalent, are the organized states achieved by microscopic organisms: amoeba aggregates [2], bacterial colonies [3, 4], and swarms of *Daphnia* [5]. Such striking self-organized collective phenomena stimulated natural extensions of trusted models and tools of equilibrium statistical mechanics to systems of coupled self-propelled particles. Proposed models have varied in degrees of idealization and complexity of the description of swarms, their environments and the interactions between them. They can be broadly divided into continuous [6–9] and discrete self-propelled particle (SPP) models [10–13], both coming in deterministic as well as stochastic varieties. In these pioneering studies, models were mainly analyzed for their ability to display certain observed phenomena (transition from swarm to flock [8, 10], vortical swarms [12, 14]), as well as the potential universality of certain features (scaling behavior [11], individual distance [15]). More often than not, they were not pushed to predictive risks that would at best qualify and refine them, at worst falsify them. While these exercises are crucial to identify generic sufficient conditions for the occurrence of observed states, they leave open the question as to whether or not these conditions necessarily obtain in the living system under investigation. In cases where such systems are open to detailed experimental investigation [4], it proves useful to explore the richness of behavior sustained by classes of models, with a view to proposing tracks for spatio-temporal evolution that might result under (slow) changes in the experimental setting. This is precisely the objective we had in mind as we embarked on our explorations, and shall dedicate the rest of this letter to describing the working model (dis-

crete, deterministic, SPP model), summarizing our extensive numerical experiments, and highlighting our significant, and eminently testable, results: a- novel types of self-organisation namely the *disk*, *ring*, *polarized vortex*, *droplet* and *expansion* states; b- a phase diagram which distills, on a reduced parameter plane, the various states, and the transitions between them; c- an intriguing route to flocking, which obtains in the presence of an external, uniform, force field.

Given the inherent complexity of our undertaking, we opted for a simple, but fairly versatile, deterministic SPP model, flavors of which have been examined by Levine *et al.* [12], in their quest for vortices, and Edelstein-Keshet *et al.* [15] in a study of individual distances in swarms. The particles in this model are identical in their mass, and in the nature of the forces they feel and generate. Their self-propulsion is mimicked with an acceleration of constant magnitude, acting along the direction of motion. They are coupled via a double exponential potential force field, which attracts at large distances, and repels at small distances. Furthermore, they are subjected to a drag force, which captures the reaction of the viscous medium in which they move (and which is here assumed linear in the velocity). Newton’s equation for the i th particle reads

$$m \frac{d\vec{v}_i}{dt} = \sigma \hat{v}_i - \gamma \vec{v}_i - \nabla_{\vec{r}_i} \phi \quad (1)$$

where m , \vec{r}_i and \vec{v}_i are the mass, position and velocity of the i th particle, σ the magnitude of the self-propulsion force, which acts along the direction of motion \hat{v}_i , and γ the friction coefficient. The potential energy ϕ is given by

$$\phi = \sum_{\substack{i,j=1 \\ j \neq i}}^N W_r \exp(-|\vec{r}_i - \vec{r}_j|/l_r) - W_a \exp(-|\vec{r}_i - \vec{r}_j|/l_a) \quad (2)$$

where N is the population size, and W_r , W_a , l_r and l_a determine the strength and range of repulsive and attractive forces respectively. It proves useful to work with the dimensionless variables $\vec{r}' = \vec{r}/l_r$, $\vec{v}' = \vec{v}/v_t$, and $t' = t/\tau$, with $v_t = \frac{\sigma}{\gamma}$ (the “terminal velocity”), and $\tau = l_r/v_t = l_r\gamma/\sigma$. In the primed variables, the equation of motion becomes

$$R \frac{d\vec{v}'_i}{dt'} = \hat{v}'_i - \vec{v}'_i + \sum_{\substack{j=1 \\ j \neq i}}^N [Q \exp(-|\vec{r}'_i - \vec{r}'_j|) - P \exp(-|\vec{r}'_i - \vec{r}'_j|/\lambda)] \hat{r}'_{ij} \quad (3)$$

with $\hat{r}'_{ij} = [\vec{r}'_j - \vec{r}'_i]/|\vec{r}'_j - \vec{r}'_i|$. We recover four dimensionless parameters: $\lambda = l_r/l_a$ (repulsive over attractive length scale, < 1), $P = W_a/\sigma l_a$ (attraction over self-propulsion), $Q = W_r/\sigma l_r$ (repulsion over self-propulsion), and $R = m\sigma/(l_r\gamma^2)$ (a Reynolds-like number for the flow), which together with the population size N , fully specify a swarm in our model.

In what follows, we are primarily concerned with the behavior of 2D swarms. Initially (and except when otherwise specified), particles are uniformly distributed in a square (its size being chosen so that the initial swarm is bounded [16]), with randomly oriented initial velocities, and speeds uniformly distributed between 0 and the terminal velocity. Populations ranging in size between 100 and 1000 members were considered. With these initial conditions, and the help of a 4th order, adaptive, Runge-kutta scheme [17], we thoroughly explored the parameter space. Simulations were allowed to run till the system’s energy (and wherever relevant, mean velocity and density) relaxed to near steady configurations, on which our classification is based. Results are viewed in the center of mass frame, the origin of which, though interesting in its wanderings, is not a serious concern of this inquiry.

Broadly speaking, these random initial conditions converge, to a center manifold (think of it as the terminal velocity manifold), on which the swarm relaxes to distinct regimes, which though not exhaustive of the rich behavior allowed by this model, constitute the skeleton on which a complete description will be eventually fleshed out. Before displaying, then analyzing, a typical (two dimensional) space in which these regimes find their proper home, we survey their main qualitative properties. We draw our results from experiments with 1000 particles, while noting that the existence and main qualitative properties of these regimes are independent of the size of the population.

We start with the *ring* state, shown in Fig. 1(a), a highly regimented configuration, in which particles rotate and counter-rotate on a perfect circle. Next in line, is the *polarized vortex*, shown in Fig. 1(b), in which nearly all particles travel in the same direction [18]. A hitherto unsuspected formation is the *droplet* state, Fig. 1(c-d), in which the swarm breaks up into a necklace of drop-like flocks. Droplets rotate clockwise and counter-

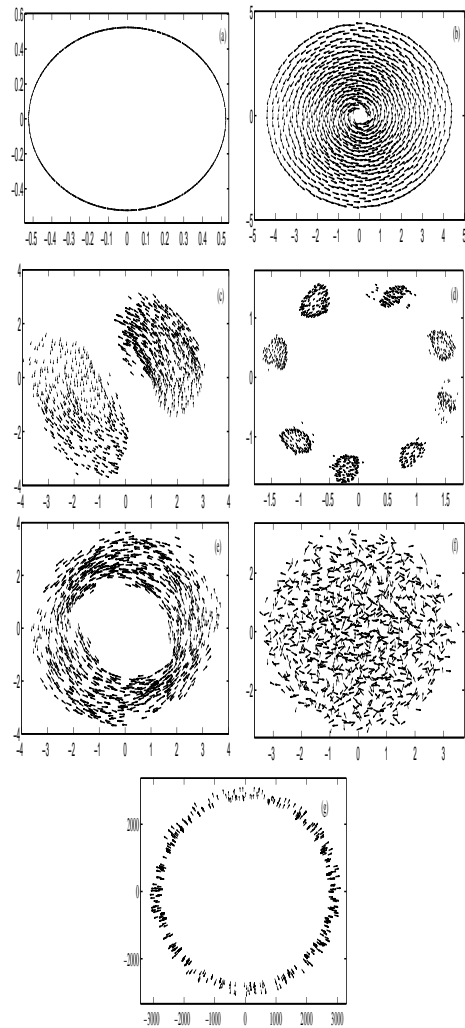


FIG. 1: Steady states, for $N = 1000$, $\lambda = 2/3$, and $P = 0.1$: (a) Ring State, $Q = 0.1$ and $R = 3$. (b) Polarized vortex, $Q = 0.21$ and $R = 0.0975$. (c) and (d) Droplet states, with $Q = 0.1575$, $R = 3.75$ and $Q = 0.1125$, $R = 7.5$ respectively. (e) Vortex state, $Q = 0.15$ and $R = 5.625$. (f) Disordered Disk State, $Q = 0.1875$ and $R = 0.0375$; (g) Expansion State, $Q = 0.2625$ and $R = 0.375$.

clockwise, with near constant angular velocity, holding tight through repeated mergers with fellow droplets traveling in the opposite direction. Bona fide *vortices*, on which particles are nearly split even between prograde and retrograde circulation, are shown in Fig. 1(e). Fig. 1(f) shows an example of the disordered *disk* state, in which particles move chaotically, while self-confined within a disk like region. Lastly, the *expansion* state, in which self-propulsion dominates over attractive forces to promote the outward explosion of the swarm, is shown in Fig. 1(g).

Perhaps more important than the identification of novel self-organized states, is the realization that the

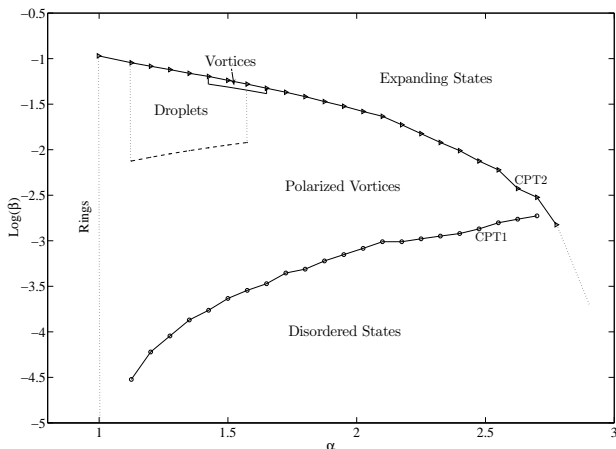


FIG. 2: The phase diagram, for $N = 1000$, and $\lambda = 2/3$. $\beta = R/NP$ is plotted against $\alpha = Q/P$. The dotted $\alpha = 1$ line, the line of *rings*, separates the multi-swarm (attraction dominated) region to its left, from the swarm dynamics regions to its right. Circles mark transitions from disordered *disk* to *polarized vortex* state; triangles mark transitions from ordered to *expansion* state.

five dimensional parameter space (the four dimensionless model parameters, plus N) reduces, once the dynamics settles on the terminal velocity manifold, to a three dimensional space, in which the variety of relaxed, self-organized configurations, is itself organized in a phase (morphology) diagram of sorts. This space is spanned by $\lambda = l_r/l_a$, $\alpha = Q/P = W_r/(\lambda W_a)$, and $\beta = R/NP = mv_t^2/(N\lambda W_a)$. We verified, with extensive numerical explorations, that models with the same (λ, α, β) relax to qualitatively similar configurations, that a steady configuration in the (λ, α, β) plane unfolds into a hyper-surface of similar configurations in the five dimensional parameter space of the model.

It was noted [19] that the Morse potential (Eq. 2) with parameter values resulting in self-organized states is not H -stable in the language of statistical mechanics [20]. H -stability is related to the existence of a well-defined thermodynamic limit with finite intensive local densities. The system which is not H -stable is called catastrophic. Indeed, the necessary criterion to ensure this stability is that the integral over space of the pair interaction potential be non-negative. Since

$$\int \phi(r) d^2r = 2\pi W_a l_a^2 (\alpha \lambda^3 - 1)$$

the criterion is not satisfied and the system is catastrophic for $\alpha < \lambda^{-3}$. In the catastrophic regime the average potential energy per particle in large but finite systems is proportional to N .

The reduced set of parameters has, therefore, simple physical meaning: α and λ together define the shape of the potential, and, in particular, the degree to which

the system is away from H -stability. As α increases towards the value of λ^{-3} the system approaches the normal, non-catastrophic regime. On the other hand, β has the meaning of the ratio of the typical kinetic energy to the potential energy per particle (which is dominated by attraction and is of order NW_a).

In this reduced parameter space, one could survey steady states, and neighbouring configurations, by varying three of the model parameters (say W_a , l_a and γ or σ) and keeping the others (W_r , l_r , N and σ or γ) fixed. Thousands of computing hours went into clarifying the salient features of the resulting phase diagram, the invariant structures of the model. These features are clearly delineated on constant λ slices, where the relaxed dynamics typically splits into four regions, as apparent in the particular instance in Fig. 2: a) a region occupied by the disordered *disk* states, for smallish β (attraction and viscosity dominated models); b) a region occupied by unbound, expanding states, for largish β (propulsion dominated models); c) an intermediate region where all organized states live (i.e. rings, droplets, polarized vortices and regular vortices). This region is bounded below by the critical phase transition line (CPT1) between disordered and ordered states, and above by the critical phase transition line (CPT2) between ordered and expanding states. It is bounded to the left by the line $\alpha = 1$, or $W_a/l_a = W_b/l_b$, a line of ring states, the radius of which increases with increasing β , all else being held fixed, till the point (past CPT2) where the dominant self-propulsion fragments the ring into an expanding state; d) a region of irregular, multi-cluster, and unsteady configurations, which is obtained in attraction dominated models (to the left of the *ring* line, and which we keep out of our humble focus on coherent, relaxed swarms).

CPT1 and CPT2 meet at a crossroads between the disordered disk, the polarized vortex and the expanding state; CPT2 stretches beyond that meeting point into regimes which are held together by viscosity's countering of the mutual repulsion of particles. For $\alpha > 1$, and β just above CPT1, polarized vortices are always observed. In fact, just above CPT1, *all* particles are circulating in the same direction. Increasing β , at constant α , the number of counter rotating particles grows steadily till the polarized vortex is destabilized, in three possible ways, depending on the value of α : 1) The polarized vortex breaks up into droplets (mostly two) rotating in the same direction, with a small fraction of particles moving erratically in the opposite direction. Increasing β , the number of droplets increases, with nearly as many droplets rotating in one direction as the other. Looking at larger values of β , the droplets can either go directly to the expansion state or, and for a small α interval, they become more elongated and pass through the vortex state before breaking up and expanding. 2) The polarized vortex morphs directly into a regular vortex and then to an expanding state. 3) The polarized vortex transitions directly to

the expansion state; here, and very close to CPT2, we find mixed states—that is states in which a small fraction of particles expands while the other forms a special vortex [21]. Transitions among the organized states are harder to identify numerically, better handled through a careful stability analysis in a mean field approach to the problem, and are only roughly determined in the current study [22]. On the other hand, transitions across CPT1 and CPT2 are discontinuous, and reminiscent of the first order phase transitions of equilibrium statistical mechanics. To better clarify this character, we define an order parameter $L = \langle r|\dot{\theta}| \rangle$, the bracket indicating an average over all the particles in a given steady state. L is nearly equal to zero in the expanding state, tends to $\frac{2}{\pi} \approx 0.636$ for a completely random state, and 1 for vortex like dynamics. Following L with β , for fixed α , we observe the system in Fig. 3 undergoing the two sharp transitions, from random to organized, and from organized to expanding. For $\alpha > 2.7$, the swarm transitions directly from the *disordered* to the *expansion* state.

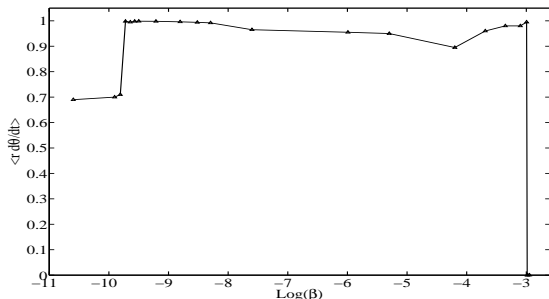


FIG. 3: The transition among CPT1 and CPT2 are shown. The order parameter $\langle r|\dot{\theta}| \rangle$ is plotted against β . The graph was obtained for $N = 1000$, $\lambda = 2/3$, and $\alpha = 1.275$.

To clarify the nature of some of the transitions observed, we undertake a study of a thermodynamic analogy of the self-propelling system.

It is clear from the phase diagram that one of the control parameters, β , has the meaning of the ratio of the typical kinetic energy to the potential energy per particle. In the thermodynamic analogy, we consider a system with exactly the same interaction, but the kinetic energy is controlled by temperature instead of the self-propulsion to viscosity ratio. Consider the canonical ensemble description of a system of N particles with pair interaction specified by Eq. 2 enclosed in a circular box of radius R and kept at temperature T . Thermodynamic properties are treated in the self-consistent field approximation. According to the standard formulation of the variational mean field theory [23] the density is related to the mean-field potential by

$$n(\vec{r}) = A \exp\left(\frac{-\varphi_{mf}(\vec{r})}{T}\right)$$

where A is determined by normalization

$$N = \int n(\vec{r}) d^2r$$

and the mean-field potential is given by

$$\varphi_{mf}(\vec{r}) = \int n(\vec{r}') \phi(\vec{r}' - \vec{r}) d^2r'$$

Axial symmetry was assumed, and self-consistent field equations were solved numerically by an iterative procedure for various temperatures and interaction parameter α at fixed $\lambda=2/3$. In a fairly broad temperature range two stable solutions exist: one with an almost uniform low density, corresponding to the gas phase, and the other with a large density near the center and extremely low density at the periphery, corresponding to the liquid droplet phase. Intriguingly, stable droplet solutions exist only within the catastrophic regime $\alpha < (3/2)^3$.

In order to analyze thermodynamic stability we calculate the Helmholtz free energy for each solution (phase) in the same self-consistent field approximation:

$$F = \frac{1}{2} \int n(r)n(r')\phi(|\vec{r} - \vec{r}'|)d^2rd^2r' + \\ + T \int n(r) \ln(n(r)/N) d^2r$$

The velocity-related contribution is the same for both phases and will not be considered explicitly. The solution with the lower free energy corresponds to thermodynamic equilibrium while the other solution can be associated with a metastable phase. Upon approaching certain temperature, a solution may lose its iterative stability and eventually disappear. In the language of thermodynamics, this would mean reaching the spinodal line. Temperature dependence of the two branches of the free energy is shown in Fig. 4(a).

The fact that two branches of the free energy cross is typical of classical first order transitions. However, in contrast to standard situations simultaneous coexistence of two phases is impossible. Each of the two solutions describes the system as a whole while, say, a 50-50 mixture of uniform gas and liquid droplet is not a self-consistent solution at all. This is why the transition temperature is defined from the condition that the two phases have equal total free energies rather than from equality of chemical potentials. We recall that another distinction of the current situation is that a standard thermodynamic limit is not very meaningful. However, from a pragmatic point of view, first order transitions in finite systems can still be defined if there are two distinct states with the free energies that are large on the T scale and cross as functions of some control parameter. Phase transitions in an isolated macromolecule are conceptually close to the situation studied here, [24]

We make a connection with the dynamic system by equating mv_t^2 and T (Boltzmann constant is 1) since

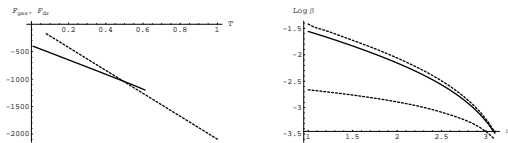


FIG. 4: (a) Temperature dependence of the two branches of the free energy: liquid droplet phase (solid line) and gas phase (dotted line) for $N = 1000$, $\lambda = 2/3$, $\alpha = 2.85$. The lines terminate at respective spinodal points. T is expressed in W_a units. (b) Phase diagram of the thermodynamic system for $N = 1000$, $\lambda = 2/3$, box radius $R = 30l_a$, in the same coordinates as in Fig 2. The equilibrium transition line is solid, spinodal lines are dashed. The liquid droplet phase is stable below the transition line, and metastable in the range between the solid and the upper dashed lines.

the system is 2-dimensional, so that $\beta = T/N\lambda W_a$. The transition line in the $(\alpha, \text{Log}\beta)$ coordinates is presented in Fig. 4(b) together with two spinodal lines for $N=1000$, $\lambda=2/3$, and $R = 30l_a$. Separate calculations with a different number of particles $N=500$ confirm that our choice of β and α as scaling parameters yield a universal N -independent phase diagram. There is a weak (logarithmic) effect of the box radius R on the transition temperature which is naturally related to the entropy of the gas phase, but further elaboration of the thermodynamic model is the subject of future work.

It is clear that the gas-droplet transition line resembles closely the CPT2 line separating the expanding and the ordered states. This gives a strong support to the claim that the transitions in the dynamic system are indeed a direct analogy to phase transitions. Analysis of the dynamic analogy of the metastable thermodynamic states would involve a study of the attractor basins in the phase space and is beyond the scope of the present paper. The thermodynamic system does not support dynamically organized states, nor do we observe a transition analogous to the CPT1 line. A system of self-propelled particles can be highly organized in the momentum space which is impossible for a classical system of interacting particles in the canonical ensemble where Maxwell's distribution is unavoidable. Note, however, that the current statements concerning the thermodynamic system are based only on the results of the self-consistent field approximation, while the true ordering in the coordinate space may be more intricate.

We conclude our discussion of critical phase transitions with a brief mention of an interesting phenomenon, which is analogous to the notorious swarm to flock transition, and which, unlike the self-promoted transitions seen in this and other instances in the literature, occurs in the presence of an external, uniform, force field. Fig. 5 (b) shows a *polarized* flock in which all particles are traveling with the same velocity, a state which resulted by subjecting a *disordered* disk state of our model (seen in Fig. 5

(a)) to a constant, external force field. Such a polarized flock does not emerge for any field strength. In fact, a discontinuous transition, from random to polarized, occurs as the strength of the external field, \vec{f}_{ext} , is increased past a critical value (which naturally depends on the initial phase of the swarm (i.e. on the swarm's λ, α , and β). The center of mass speed: $\omega = |\sum_{i=1}^N \vec{v}_i| / (Nv_{max})$ (normalized by v_{max} , the maximum speed in the swarm), is a suitable order parameter for the transition from *disordered* disk ($\omega = 0$), to *polarized* flock ($\omega = 1$), which is clearly illustrated in Fig. 5(c).

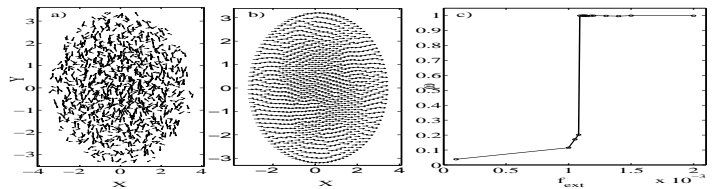


FIG. 5: The transition from disordered swarm to an aligned flock: a) Shows the initial disordered state; b) Shows the steady solution after applying the external field ($f_{ext} = 0.00115$); c) shows the 1st order phase transition where we plot the order parameter ω vs the external field strength (normalized by self-propulsion σ). The graphs were obtained for $N = 1000$, $\lambda = 2/3$, $\alpha = 1.875$ and $\beta = 5.25 \times 10^{-5}$.

In summary, we have succeeded in constructing a phase diagram that captures, in one fell swoop, the global structure of steady 2D configurations, in a deterministic model of coupled self-propelled particles. Through a systematic numerical exploration of the model's parameter space, we have identified novel types of collective behavior such as *rings*, *droplets*, *special vortices*, *disordered* disks, and *expanding* states; we have shown that transitions from disordered to ordered, then from ordered to expanding state, have the structure of discontinuous, "first order", phase transitions (in line with the results of [25], which attribute the continuous transitions reported by [10] to finite-size effects); we have supported the phase transition analysis by studying a thermodynamic analogy where a temperature-driven transition from a gas to a condensed liquid droplet is observed and matches closely the transition from ordered to expanded state; finally, we have shown that a *disordered* swarm, when subjected to an external uniform field, transitions to a *polarized* flock, once again in a discontinuous manner. The genericity of discontinuous phase transitions, the stability and evolution of organized states, the surface tension and shape dynamics of swarms, are the subject of ongoing work. In the mean time, the constructed phase diagram offers a promising geography for experimental verification, and refinement, or at worst, falsification of this class of models. In particular, the same bacteria which stimulated an

earlier investigation of model vortices [12], could perhaps be stimulated into transitions from disordered motion, to polarized vortex, to droplets, or vortex, by judicious selection and control of population size, medium resistance, concentrations of chemo-attractants/repellents, external drivers...etc. As evident in Fig. 2, an order of magnitude increase in population size (decrease in β) is expected to bring about the disintegration of a colony, initially organized in a polarized vortex, into a disordered disk, and this over a range of interaction potentials (of α s); similar effects could result from a slowing down of particles in the colony (through increased friction and/or reduced self-propulsion); an increasing concentration of chemo-attractants (a decreasing α) may push an initially vortical colony closer to a *ring* state [26]. We look forward to exchanges with experimentalists around this model's phase diagram, in the hope that similar systematic (not to say exhaustive) explorations of macroscopic phases of collective motion in the lab, together with the model improvements that they will surely stimulate, may eventually pave the way to a refined characterization of the notoriously elusive (at times microscopic) mechanical properties of coupled, self-propelled living organisms.

* Electronic address: jt00@aub.edu.lb

† Electronic address: amer.shreim@gmail.com

- [1] J. Parrish and L. Edelstein-Keshet, *Science* **284**, 99 (1999).
- [2] W.-J. Rappel, A. Nicol, A. Sarkissian, and H. Levine, *Physical Review Letters* **83**, 1247 (1999).
- [3] E. Ben-Jacob, I. Cohen, A. Czirok, T. Vicsek, and D. L. Gutnick, *Physica A* **238**, 181 (1997).
- [4] A. M. Delprato, A. Samadani, A. Kudrolli, and L. Tsimering, *Physical Review Letters* **87** (2001).
- [5] A. Ordemann, G. Balazsi, and F. Moss, *Physica A* **325**, 260 (2003).
- [6] A. Mogilner and L. Edelstein-Keshet, *Journal of Mathematical Biology* **38**, 534 (1999).
- [7] G. Flierl, D. Grunbaum, S. Levin, and D. Olson, *Journal of Theoretical Biology* **196**, 397 (1999).
- [8] J. Toner and Y. Tu, *Physical Review Letters* **75**, 4326 (1995).
- [9] J. Toner and Y. Tu, *Physical Review E* **58**, 4828 (1998).
- [10] T. Vicsek, A. Czirok, E. Ben-Jacob, I. Cohen, and O. Shochet, *Physical Review Letters* **75**, 1226 (1995).
- [11] A. Czirok and T. Vicsek, *Physica A* **281**, 17 (2000).
- [12] H. Levine, W.-J. Rappel, and I. Cohen, *Physical Review E* **63** (2000).
- [13] N. Shimoyama, K. Tsuyoshi, Y. Hayakawa, and M. Sano, *Physical Review Letters* **76**, 3870 (1996).
- [14] R. Mach, A. Ordemann, and F. Schweitzer, *Journal Of Theoretical Biology* **1000** (2004).
- [15] A. Mogilner, L. Edelstein-Keshet, L. Bent, and A. Spiros, *Journal of Mathematical Biology* **47**, 353 (2003).
- [16] Refer to [27] for details.
- [17] W. H. Press, S. A. Teukolsky, W. T. Vetterling, and B. P. Flannery, *Numerical Recipes in C++* (Cambridge University Press, 2002), 2nd ed.
- [18] In [12], a *polarized* vortex is obtained by forcing polarized initial conditions; here it arises naturally from random initial conditions.
- [19] M. D'Orsogna, Y. Chuang, A. Bertozzi, and L. Chayes, *Physical Review Letters* **96**, 104302 (2006).
- [20] D. Ruelle, *Statistical Mechanics: Rigorous Results* (World Scientific, 1999).
- [21] All the states referred to here are steady states solutions reached by starting from random initial conditions, and not by following a relaxed state with slowly changing parameters.
- [22] The ring state (existence, radius, and stability) is nicely handled in a mean-field approach, through which the dynamics reduces to that of coupled limit cycles (see [27] for further details). These results along with, a more elaborate treatment of the dynamics of coupled limit cycles, the organized states that are captured through it, and their stability analysis, will constitute the subject of an upcoming work [28].
- [23] P. Chaikin and T. Lubensky, *Principles of Condensed Matter Physics* (Cambridge University Press, 2000).
- [24] L. Klushin, A. Skvortsov, and F. Leermakers, *Physical Review E* **69**, 061101 (2004).
- [25] G. Gregoire and H. Chate, *Physical Review Letters* **92**, 25702 (2004).
- [26] The experiments of [4] in which, interestingly enough, bacterial colonies evolve from a disk into a *ring* state when exposed to UV radiation, offer a promising setting in which the evolution of phases of collective motion with population size, medium resistance and chemoattractant concentration, may be fruitfully studied.
- [27] A. Shreim, Master's thesis, American University of Beirut (2004).
- [28] J. Touma, B. Fayyad, and A. Shreim, in Preparation.

